Achievable Sum Rate and Outage Capacity of GFDM Systems with MMSE Receivers

Carrillo Dick, Kumar Santosh, Fraidenraich Gustavo, Nardelli Pedro H. J., da Costa Daniel B.

DOI: 10.1109/ICC40277.2020.9149450

Achievable Sum Rate and Outage Capacity of GFDM Systems with MMSE Receivers

Dick Carrillo[1], Santosh Kumar[2], Gustavo Fraidenraich[3], Pedro H. J. Nardelli[1], and Daniel B. da Costa[4]
[1]School of Energy Systems, LUT University, Finland
[2]Department of Physics, Shiv Nadar University, India
[3]School of Electrical and Computer Engineering, State University of Campinas, Brazil
[4]Department of Computer Engineering, Federal University of Ceará, Brazil

***Abstract*—This paper investigates the achievable sum rate and the outage capacity of generalized frequency division multiplexing systems (GFDMs) with minimum mean-square error (MMSE) receivers over frequency-selective Rayleigh fading channels. To this end, a Gamma-based approximation approach for the probability density function of the signal-to-interference-plus-noise ratio is presented, based on which accurate analytical formulations for the achievable sum rate and outage capacity are proposed. The accuracy of our analysis is corroborated through Monte Carlo simulation assuming different GFDM parameters. Illustrative numerical results are depicted in order to reveal the impact of the key system parameters, such as the number of subcarriers, number of subsymbols, and roll-off factors, on the overall system performance.**

***Index Terms*—Achievable sum rate, GFDM systems, outage capacity, MMSE receivers.**

I. Introduction

Along the last years, Generalized Frequency Division Multiplexing (GFDM) has arisen as a potential alternative to Orthogonal Frequency Division Multiplexing (OFDM) for beyond 5G systems due to its promising bandwidth efficiency improvements [1]. Specifically, GFDM filters each subcarrier with a well-localized prototype filter and has low out-of-band (OOB) emission [2]. GFDM is also designed with a cyclic prefix (CP) that can be used by a large number of transmitted symbols instead of appending a CP per symbol, as in the OFDM case [3]. It has also been shown that GFDM can be harmoniously integrated with multiple-input multiple-output (MIMO) channels [2].

Despite of the above attractive features, GFDM has some deficiencies. In particular, it leads to self-interference among the transmitted symbols, which needs be equalized using, for instance, linear receivers as minimum mean square error (MMSE) to recover individual input samples from channel output. In this case, MMSE has the advantage of having low complexity compared to other non-linear receivers. However, fundamental performance limits of such an interesting combination, i.e., GFDM and MMSE receivers, are still unknown. Moreover, the current available literature dealing with GFDM systems only provides a handful of studies dealing with the sum rate of these systems. For instance, Seungyul *et al.* in [4] derived the data rates of GFDM systems for two types of channels: additive additive white Gaussian noise (AWGN) channel and Long-Term Evolution (LTE) Pedestrian B channel. However, such results relied on numerical approaches that were only valid for specific scenarios, limiting their generalization and practical usefulness.

Aiming to fill partly the gap that exists in the literature, this paper investigates the achievable sum rate and outage capacity of GFDM systems employing MMSE receivers and undergoing frequency-selective Rayleigh fading. To this end, a Gamma-based approximation approach for the probability density function (PDF) of the signal-to-interference-and-noise ratio (SINR) is presented, based on which, accurate analytical formulations are attained. The idea behind the proposed approximation relies on the framework proposed in [5]. The accuracy of our analysis is corroborated through Monte Carlo simulation assuming different GFDM parameters. Illustrative numerical results are depicted in order to reveal the impact of the key system parameters, such as number of subcarriers, number of subsymbols, and roll-off factors, on the overall system performance. To the best of the authors' knowledge, our theoretical results have not been reported in the literature yet and they can be used as a benchmark for future wireless communication studies.

The remainder of the paper is organized as follows. Section II describes the system model along with specific details for the transmitter and receiver blocks. Section III extends the description of the Gamma-based approximation approach proposed in [5], and applies it subsequently in Sections IV and V to derive closed-form accurate approximations for the achievable sum rate and the outage capacity, respectively. Section VI presents illustrative numerical results, which are corroborated by means of Monte Carlo simulations. Finally, Section VII concludes the paper.

II. System Model

The considered GFDM system setup is designed to transmit a complex symbol block $d_{s,k}$ at the sth time instant and kth subchannel containing $S \times K$ data symbols ($s = 0, \ldots, S-1$; $k = 0, \ldots, K-1$). Assuming that the data symbols are independent and identical, the GFDM signal can be written as

$$x[n] = \sum_{s=0}^{S-1} \sum_{k=0}^{K-1} d_{s,k}\ g_{s,k}[n], \tag{1}$$

where $g_{s,k}[n]$ denotes the circular time-frequency shifted version of the prototype filter $g[n]$, being expressed as

$$g_{s,k}[n] \triangleq g[(n - sK)_N]\ e^{j2\pi nk/K}, \tag{2}$$

where $N = S \times K$ and $(.)_N$ stands for modulo operator. To simplify the circular convolution, the transmitter filter $g[n]$ is usually designed as being circular with a period of n mod N. Also, it is noteworthy that in (2) the GFDM shifting step is K in time domain and $1/K$ in frequency domain. Next, the transmitter and receiver blocks of the considered GFDM system setup will be described.

A. Transmitter Block

Let us first use (1) to rewrite the elements of the transmit symbol block in a single vector as: $\mathbf{d} = [\mathbf{d}_0^T, \dots \mathbf{d}_{s-1}^T]^T$ and $\mathbf{d}_s = [\mathbf{d}_{s,0}, \dots \mathbf{d}_{s,K-1}]^T$, with variance σ_{d}^2. The vector form of $x[n]$ $(n = 0, \dots, N-1)$ can be formulated as

$$\mathbf{x} = \mathbf{A}\mathbf{d}, \tag{3}$$

where $\mathbf{x} = [x[0], \dots x[N-1]]^T$ and $\mathbf{A}$, with dimension $N \times N$, denotes the modulation matrix or self-interference matrix of the GFDM system. This matrix can be defined as $\mathbf{A} = [\mathbf{G}_0, \dots \mathbf{G}_{S-1}]$ so that $\mathbf{G}_s$ represents the $N \times K$ matrix of $g_{s,k}[n]$ coefficients, i.e.,

$$\mathbf{G}_s = \begin{bmatrix} g_{s,0}[0] & g_{s,1}[0] & \cdots & g_{s,K-1}[0] \\ g_{s,0}[1] & g_{s,1}[1] & \cdots & g_{s,K-1}[1] \\ \vdots & \vdots & \ddots & \vdots \\ g_{s,0}[N-1] & g_{s,1}[N-1] & \cdots & g_{s,K-1}[N-1] \end{bmatrix}. \tag{4}$$

A CP of length N_{cp} is added to the GFDM signal $\mathbf{x}$ to prevent inter-block interference over frequency selective fading channel (FSFC). Then, the transmitted signal is given by $\mathbf{x}_{\text{cp}} = [\mathbf{x}(N - N_{\text{cp}} + 1 : N);\ \mathbf{x}]$.

B. Receiver Block

Without any loss of generality, we assume a zero-mean circular symmetric complex (ZMCSC) Gaussian channel $\mathbf{h} = [h_1, h_2, \cdots, h_L]^T$, where h_r denotes the complex baseband channel coefficient of the rth path $(1 \le r \le L)$. Consider also that $N_{\text{cp}} \ge L$, which means that the CP length must be higher than the delay spread of the multipath channel [6]. Additionally, the channel coefficients related to distinct paths are assumed uncorrelated. Then, the received signal has length $N_{\text{t}} = N_{\text{cp}} + N + L - 1$ and can be modeled as

$$\mathbf{y}_{cp} = \mathbf{h} * \mathbf{x}_{\text{cp}} + \boldsymbol{\nu}_{\text{cp}}, \tag{5}$$

where the symbol $*$ symbolizes linear convolution operation, $\boldsymbol{\nu}_{\text{cp}}$ is the AWGN signal with variance σ_ν^2 and it is also represented by a vector of length N_{t}.

Before starting decoding process, the CP introduced at the transmitter needs to be removed. The frequency-domain equalization (FDE) properties can be employed so that the linear convolution in (5) becomes a circular convolution. So, the resulting received vector after CP removal can be expressed as

$$\mathbf{y} = \mathbf{H}_{\text{ch}}\boldsymbol{A}\mathbf{d} + \boldsymbol{\nu}, \tag{6}$$

where vector $\boldsymbol{\nu}$ represents the AWGN signal of length N with variance σ_ν^2 and $\mathbf{H}_{\text{ch}}$ is the $N \times N$ circular Toeplitz matrix based on vector $\mathbf{h}$, and can be written as[7]:

$$\mathbf{H}_{\text{ch}} = \begin{bmatrix} h_1 & 0 & \cdots & 0 & h_L & \cdots & h_2 \\ h_2 & h_1 & \cdots & 0 & 0 & \cdots & h_3 \\ \vdots & & \ddots & & & \cdots & \vdots \\ h_L & h_{L-1} & \cdots & \cdots & \cdots & \cdots & 0 \\ 0 & h_L & \cdots & \cdots & \cdots & \cdots & 0 \\ \vdots & & \ddots & & & \cdots & \vdots \\ 0 & 0 & & h_L & \cdots & \cdots & h_1 \end{bmatrix}. \tag{7}$$

The matrix $\mathbf{H}_{\text{ch}}$ has a very special pattern. Specifically, every row is the same as the previous row, just shifted to the right by 1 (wrapping around "cyclically" at the edges). That is, each row is a circular shift of the first row. To estimate the transmitted complex data symbols $\hat{\mathbf{d}}$, we consider a matrix $\mathbf{G}$ using the following relationship

$$\hat{\mathbf{d}} = \mathbf{G}\ \mathbf{y}, \tag{8}$$

where $\mathbf{G}$ denotes the MMSE receiver matrix.

Mathematically, the MMSE receiver matrix $\mathbf{G}$ is defined by the following:

$$\mathbf{G} = (\mathbf{H}_{\text{ch}}\mathbf{A})^\dagger\ (p\mathbf{I}_N + (\mathbf{H}_{\text{ch}}\mathbf{A})^\dagger(\mathbf{H}_{\text{ch}}\mathbf{A}))^{-1}, \tag{9}$$

where the operator $(.)^\dagger$ represents the Hermitian-conjugate of a matrix, $\mathbf{I}_N$ is a $N \times N$ identity matrix, and p is the average signal-to-noise ratio (SNR), given by $p = \sigma_d^2/\sigma_\nu^2$. Based on the MMSE receiver, it can be shown that the SINR of the nth data symbol can be expressed as

$$\Gamma_n = \frac{1}{\text{MMSE}_n} - 1 = \frac{1}{\left[(\mathbf{I}_N + \frac{p}{N}(\mathbf{H}_{\text{ch}}\mathbf{A})^\dagger\mathbf{H}_{\text{ch}}\mathbf{A})^{-1}\right]_{nn}} - 1. \tag{10}$$

Note that (10) has the same form of [8, Eq. (7.49)], being therefore not restricted to binary signals and its derivation is based on the second-order statistics of the input signals [9].

III. Approximation Approach for Γ_n

By analyzing (10), it can be verified that the product $\mathbf{H}_{\text{ch}}\mathbf{A}$ is not a circular matrix. In this case, a closed-form expression for the joint PDF of the eigenvalues seems unfeasible. However, an accurate approximation for such statistics has been previously proposed in [5]. This approximation follows some assumptions that are described in the following subsections. Firstly, we will describe how the joint PDF of the eigenvalues of the matrix $\mathbf{H}_{ch}$ is obtained. Then, we will provide further insights on how to obtain the joint PDF of the eigenvalues of the matrix $\mathbf{H}_{ch}\mathbf{A}$. Finally, we will describe the procedure to obtain the approximation of the PDF of the SINR of Γ_n, which will be based on a Gamma approximation.

A. Joint Probability Density of Eigenvalues of $\mathbf{H}_{ch}$

Let us consider a general matrix $\mathbf{H}$, as defined in [10], where each channel coefficient is represented by h_r $(r = 1, ..., N)$ defined by a complex Gaussian distribution with zero-mean and variance σ_r^2. Thus, the PDF of h_r (independent and identically distributed Rayleigh channel realizations) can be expressed by

$$p_{h_r}(h_r) = \frac{1}{2\pi\sigma_r^2} \exp\left(-\frac{|h_r|^2}{2\sigma_r^2}\right). \tag{11}$$

The matrix $\mathbf{H}$ is defined as

$$\mathbf{H} = \begin{bmatrix} h_1 & h_N & \cdots & h_2 \\ h_2 & h_1 & \cdots & h_3 \\ \vdots & \vdots & \cdots & \vdots \\ h_N & h_{N-1} & \cdots & h_1 \end{bmatrix}. \tag{12}$$

From probability theory concepts, it can be shown that the joint PDF of $\{h_1 \ldots, h_N\}$ can be expressed as

$$p_{\mathbf{h}}(h_1, ..., h_N) = \prod_{r=1}^{N} \frac{1}{2\pi\sigma_r^2} \exp\left(-\frac{|h_r|^2}{2\sigma_r^2}\right). \tag{13}$$

Following the property of circulant matrices, as the one expressed in (12), the normalized eigenvectors are always the same [10]. Thus, the normalized k-th eigenvector $\mathbf{v}^{(k)}$, where $k = 0, 1, \ldots, N-1$, can be expressed as

$$\mathbf{v}^{(k)} = \frac{1}{\sqrt{N}} \left(\omega_N^{0k}\ \omega_N^{1k}\ \omega_N^{2k}\ \ldots\ \omega_N^{(N-1)k}\right)^T, \tag{14}$$

In this case, the variables ω_N^{jk} can be determined as

$$\omega_N^{jk} = e^{\frac{2\pi i}{N} jk}, \tag{15}$$

where i represents the imaginary unit, and $j = 0, 1, \ldots, N-1$. Note that (15) represents the Nth root of unity.

By its turn, the matrix $\mathbf{F}$, whose columns are the eigenvectors, can be defined as

$$\mathbf{F} = \left(\mathbf{v}^{(0)}\ \mathbf{v}^{(1)}\ \mathbf{v}^{(2)}\ \ldots\ \mathbf{v}^{(N-1)}\ \right), \tag{16}$$

which has the following entries

$$\mathbf{F}_{jk} = \mathbf{v}_j^{(k)} = \omega_N^{jk}. \tag{17}$$

Note that the operation of multiplying a vector by matrix $\mathbf{F}$ represents the discrete Fourier transform (DFT) of that vector. With this in mind, we can define the vector $\hat{\mathbf{c}}$ as

$$\hat{\mathbf{c}} = \mathbf{F}\mathbf{c} = \left(\lambda_0^*, \lambda_1^*, \lambda_2^*, \ldots, \lambda_{N-1}^*\right), \tag{18}$$

where $\mathbf{c}$ denotes the first row of $\mathbf{H}$, and $\hat{\mathbf{c}}$ stands for the DFT of vector $\mathbf{c}$, also representing the vector composed by the eigenvalues of $\mathbf{c}$.

We proceed similarly with $\mathbf{F}$, which is also a unitary matrix, to diagonalize $\mathbf{H}$ based on the following relationship

$$\text{diag}(\lambda_j^*) = \mathbf{F}^\dagger \mathbf{H} \mathbf{F}, \tag{19}$$

where, for both cases, λ_j^* has entries defined by

$$\lambda_j^* = \sum_{k=0}^{N-1} h_k \omega_N^{kj}. \tag{20}$$

Based on the fact that each h_k is complex Gaussian distributed with zero-mean and variance σ_r^2, the complex eigenvalues λ_j^* have joint PDF being given by

$$p_{\boldsymbol{\lambda}^*}(\lambda_1^*, ..., \lambda_N^*) = \prod_{j=1}^{N} \frac{1}{2\pi\Phi_{\text{h}}^2} \exp\left(-\frac{|\lambda_j^*|^2}{2\Phi_{\text{h}}^2}\right), \tag{21}$$

where $\Phi_{\text{h}}^2 = \sum_{r=1}^{N} \sigma_r^2$, leading to a PDF that has zero-mean and variance Φ_{h}^2 for both real and imaginary parts.

Note that all the previous analysis was related to matrix $\mathbf{H}$. In order to extend the procedure to matrix channel $\mathbf{H}_{\text{ch}}$, we now consider the limit $\sigma_r \to 0$ for $r = (L+1), (L+2), \ldots, N$ so that we are able to analyze $\mathbf{H}_{\text{ch}}\mathbf{A}$. Let us first use the following relationship defined by

$$\text{diag}(\lambda_j) = \mathbf{F}^\dagger \mathbf{H}_{\text{ch}} \mathbf{F}. \tag{22}$$

To obtain the complex eigenvalues λ_j of $\mathbf{H}_{ch}$, we first define the joint PDF of the eigenvalues as

$$p_{\boldsymbol{\lambda}}(\lambda_1, ..., \lambda_N) = \prod_{j=1}^{N} \frac{1}{2\pi\Phi^2} \exp\left(-\frac{|\lambda_j|^2}{2\Phi_2}\right). \tag{23}$$

Then, we can finally write the variance of matrix $\mathbf{H}_{\text{ch}}$ as $\Phi^2 = \sum_{r=1}^{L} \sigma_r^2$.

B. Joint Probability Density of the Eigenvalues of $\sqrt{p}\,\mathbf{H}_{ch}\mathbf{A}$

By inspection, one can notice that the product $\mathbf{H}_{\text{ch}}\mathbf{A}$ is not necessarily a circulant matrix. Let us consider the main product factor of (10) that is represented by $p\,(\mathbf{H}_{\text{ch}}\mathbf{A})^\dagger \mathbf{H}_{\text{ch}}\mathbf{A}$, which is an Hermitian matrix. We can employ a singular value decomposition strategy so that

$$\sqrt{p}\,\mathbf{H}_{\text{ch}}\mathbf{A} = \mathbf{V}\mathbf{M}\mathbf{U}, \tag{24}$$

where $\mathbf{V}$ and $\mathbf{U}$ are unitary matrices, and $\mathbf{M} = \text{diag}(\mu_1, ..., \mu_N)$ contains the singular values of $\sqrt{p}\,\mathbf{H}_{\text{ch}}\mathbf{A}$. From (24), we obtain

$$p\,(\mathbf{H}_{\text{ch}}\mathbf{A})^\dagger \mathbf{H}_{\text{ch}}\mathbf{A} = \mathbf{U}\mathbf{M}^\dagger\mathbf{M}\mathbf{U}^\dagger, \tag{25}$$

since $\mathbf{V}^\dagger\mathbf{V} = \mathbf{I}$.

From (10), Γ_n can be rewritten in terms of α_n so that

$$\Gamma_n = \frac{1}{\alpha_n} - 1, \tag{26}$$

where α_n is defined based on (25) as

$$\begin{aligned} \alpha_n &= \left[\left(\mathbf{I} + \frac{p}{N}(\mathbf{H}_{\text{ch}}\mathbf{A})^\dagger \mathbf{H}_{\text{ch}}\mathbf{A}\right)^{-1}\right]_{nn} \\ &= \left[\mathbf{U}\left(\mathbf{I} + \frac{1}{N}\mathbf{M}^\dagger\mathbf{M}\right)^{-1}\mathbf{U}^\dagger\right]_{nn}. \end{aligned} \tag{27}$$

Using summation notation, (27) can be re-expressed by

$$\alpha_n = \sum_{r,s=1}^{N} \mathbf{U}_{nr}\Big(1+\frac{1}{N}|\mu_r|^2\Big)^{-1}\delta_{rs}\mathbf{U}^*_{ns}, \tag{28}$$

or by

$$\alpha_n = \sum_{r=1}^{N} \Big(1+\frac{1}{N}|\mu_r|^2\Big)^{-1}|\mathbf{U}_{nr}|^2. \tag{29}$$

Based on the condition that $\mathbf{H}_{\text{ch}}\mathbf{A}$ is a circulant matrix, then $\mathbf{U}$ holds same condition as the DFT matrix given by (19) and (14). As a result, the square of the absolute value of $\mathbf{U}_{nr}$, represented by $|\mathbf{U}_{nr}|^2$, is equal to $1/N$. In this case, the eigenvalue $\{\mu_r\}$ equals to the product of $\sqrt{p}$, eigenvalues of $\mathbf{H}_{\text{ch}}$, and eigenvalues of $\mathbf{A}$. Consequently, α_n can be approximated by

$$\begin{aligned}\alpha_n &\approx \sum_{r=1}^{N} \Big(1+\frac{1}{N}|\mu_r|^2\Big)^{-1}\,\Big|\frac{1}{\sqrt{N}}\Big|^2 \\ &\approx \sum_{r=1}^{N}\frac{1}{N+|\mu_r|^2}.\end{aligned} \tag{30}$$

As properly demonstrated in [5], this assumption holds very well for different parameter configurations of matrix $\mathbf{A}$, including different roll-off factors of prototype filter $g[n]$.

Based on above, the symmetrized joint PDF of $\{\mu_j\}$, $j = 0, 1, \ldots, N-1$), can be accurately approximated by

$$\begin{aligned}p_{\boldsymbol{\mu}}(\mu_1,...,\mu_N) \approx \frac{1}{N!}\sum_{\{q(j)\}}\Bigg[\prod_{j=1}^{N}\frac{1}{2\pi p\Phi^2|\chi_{q(j)}|^2} \\ \times\exp\left(-\frac{|\mu_j|^2}{2p\Phi^2|\chi_{q(j)}|^2}\right)\Bigg],\end{aligned} \tag{31}$$

where the sum involves all $N!$ permutations of $\{q(1), q(2), ..., q(N)\}$, with $q(j)$ being the indices of $\{\chi\}$, which are the eigenvalues of the matrix A.

Now, considering the joint PDF of eigenvalues of $\sqrt{p}\,\mathbf{H}_{ch}\mathbf{A}$, as shown in Eq. (31), the next step is to find accurate approximations for the PDF of the random variables α_n and Γ_n, which will be detailed next.

C. Statistics for α_n and Γ_n

In order to compute an approximation for the PDF of α_n, we should first obtain its mean (μ) and variance (σ^2). To this end, we depart from the joint PDF given in (31) and use the relation given in (30), which results in the mean value for α_n [5]

$$\mu = \mathbb{E}[\alpha_n] = -\sum_{j=1}^{N}\left[\frac{1}{\Psi_j^2}\exp\left(\frac{N}{\Psi_j^2}\right)\text{Ei}\Big(-\frac{N}{\Psi_j^2}\Big)\right]. \tag{32}$$

We proceed similarly to compute the variance of α_n, which is given by [5]:

$$\begin{aligned}\sigma^2 &= \mathbb{E}[\alpha_n^2] - (\mathbb{E}[\alpha_n])^2 \\ &= \sum_{j=1}^{N}\Bigg[\frac{1}{N\Psi_j^2}+\frac{1}{\Psi_j^4}\exp\left(\frac{N}{\Psi_j^2}\right)\text{Ei}\Big(-\frac{N}{\Psi_j^2}\Big) \\ &\quad -\frac{1}{\Psi_j^4}\exp\left(\frac{2N}{\Psi_j^2}\right)\text{Ei}^2\Big(-\frac{N}{\Psi_j^2}\Big)\Bigg],\end{aligned} \tag{33}$$

where $\text{Ei}(x)$ represents the exponential integral function, which is defined by

$$Ei(x) = -\int_{-x}^{\infty}\frac{e^{-t}}{t}dt. \tag{34}$$

In addition, Ψ_j^2 is given by the following relation:

$$\Psi_j^2 = 2p\Phi^2|\chi_j|^2, \tag{35}$$

where $\Phi^2 = \sum_{r=1}^{N}\sigma_r^2$ and χ_j denotes the jth eigenvalue of matrix A.

Then, the PDF of α_n can be approximated in terms of the incomplete Gamma function as

$$p_\alpha(\alpha_n) \approx \frac{1}{\Gamma(k)\,\theta^k}\,\alpha_n^{k-1}\exp\left(-\frac{\alpha_n}{\theta}\right), \tag{36}$$

where $\Gamma(\cdot)$ denotes the Gamma function [11, Eq. (8.310)], $\theta = \sigma^2/\mu$, and $k = \mu^2/\sigma^2$.

Based on the approximation above, we can easily reach at an accurate approximation for the PDF of Γ_n after appropriate substitutions and using standard statistical procedure for random variables transformation, i.e.,

$$p_\Gamma(\Gamma_n) \approx \frac{1}{\Gamma(\kappa)\,\theta^\kappa}\,(1+\Gamma_n)^{-1-\kappa}\exp\left(-\frac{1}{(1+\Gamma_n)\theta}\right). \tag{37}$$

IV. Achievable Sum Rate

Assuming independent decoding at the receiver, the achievable ergodic sum rate for MMSE receiver is given by [12]:

$$\mathcal{R}^{\text{mmse}}(\Gamma_n, N) = \sum_{n=1}^{N} E_{\Gamma_n}[\log_2(1+\Gamma_n)], \tag{38}$$

which can be rewritten as

$$\begin{aligned}\mathcal{R}^{\text{mmse}} &= \sum_{n=1}^{N}\int_0^\infty [\log_2(1+\Gamma_n)]\; p_\Gamma(\Gamma_n)\; d\Gamma_n \\ &\approx \sum_{n=1}^{N}\int_0^\infty\Bigg[\log_2(1+\Gamma_n)\;\frac{1}{\Gamma(\kappa)\,\theta^\kappa}\,(1+\Gamma_n)^{-1-\kappa} \\ &\quad \exp\left(-\frac{1}{(1+\Gamma_n)\theta}\right)\Bigg]\,d\Gamma_n,\end{aligned} \tag{39}$$

to solve the Integral in (39) let $\alpha = -1/\theta$ and consider that

$$\begin{aligned}\int_0^\infty\frac{\log(x+1)}{(x+1)^p}\mathrm{d}x &= -\frac{\mathrm{d}}{\mathrm{d}p}\int_0^\infty\frac{\mathrm{d}x}{(x+1)^p} \\ &= \frac{1}{(p-1)^2}, \Re(p)>1\end{aligned} \tag{40}$$

and

$$\exp\left(\frac{\alpha}{(1+\Gamma_n)}\right) = \sum_{j\geq 0} \frac{\alpha^j}{j!\ (\Gamma_n+1)^j} \tag{41}$$

the equation for $\mathcal{R}^{\text{mmse}}$ could be re-written as

$$\begin{aligned}
\mathcal{R}^{\text{mmse}} &\approx \frac{N\ (-\alpha^\kappa)}{\Gamma(\kappa)\log(2)} \left(\sum_{j\geq 0} \int_0^\infty \frac{\log(1+\Gamma_n)}{(1+\Gamma_n)^{\kappa+1}} \frac{\alpha^j}{j!\ (1+\Gamma_n)^j} \mathrm{d}\Gamma_n \right) \\
&\approx \frac{N\ (-\alpha^\kappa)}{\Gamma(\kappa)\log(2)} \left(\sum_{j\geq 0} \frac{\alpha^j}{j!} \int_0^\infty \frac{\log(1+\Gamma_n)}{(1+\Gamma_n)^{j+\kappa+1}} \mathrm{d}\Gamma_n \right) \\
&\approx \frac{N\ (-\alpha^\kappa)}{\Gamma(\kappa)\log(2)} \left(\sum_{j\geq 0} \frac{\alpha^j}{j!}\ \frac{1}{(j+\kappa)^2} \right) \\
&\approx \frac{N\ (-\alpha^\kappa)}{\Gamma(\kappa)\log(2)} \left(\kappa^2\ {}_2F_2(\kappa,\kappa;\kappa+1,\kappa+1;\alpha) \right)
\end{aligned} \tag{42}$$

where ${}_2F_2(\cdot,\cdot;\cdot,\cdot;\cdot)$ represents the Generalized Hypergeometric function [13, pp.555-566.]. Then, using the residue theorem to the integral representation of the function $G_{p,q}^{m,n}\left(\begin{matrix} a_1,\ldots,a_p \\ b_1,\ldots,b_q \end{matrix} \middle| z \right)$, which is the Meijer's G-function [11, Eq. (9.301)] and replacing $\theta = -1/\alpha$, the Eq. (42) could be finally defined as

$$\begin{aligned}
\mathcal{R}^{\text{mmse}} \approx \frac{N}{\Gamma(\kappa)\log(2)} \Bigg(&\Gamma\Big(\kappa, \frac{1}{\theta}\Big)\Big(\log(1/\theta) + \log(\theta)\Big) + \\
&G_{2,3}^{3,0}\left(\begin{matrix} 1,1 \\ 0,0,\kappa \end{matrix} \middle| \frac{1}{\theta} \right) - \Gamma(\kappa)(\log(\theta) + \psi^{(0)}(\kappa)) \Bigg),
\end{aligned} \tag{43}$$

where $\Re(\kappa) > 0$, and $\psi^{(0)}(z) = \Gamma'(z)/\Gamma(z)$ is the Polygamma function.

V. Outage Capacity

Considering that the variable Γ_n represents the SINR, it is possible to calculate the non-ergodic capacity C_{Γ_n} of the nth data symbol by $C_{\Gamma_n} = \log_2(1+\Gamma_n)$ [14], [15]. However, to calculate the outage capacity of the system, it should be considered that there are $N = S \times K$ symbols. Then, we calculate the GFDM system capacity by

$$C_\Gamma = \sum_{n=1}^{N} \log_2(1+\Gamma_n) = N\ \log_2(1+\Gamma_n). \tag{44}$$

So, as we know the PDF of Γ_n from (37), it is possible to calculate the PDF of the random variable C_Γ, which is represented by $f_{C_\Gamma}(C_\Gamma)$ and computed using random variable transformation, i.e.,

$$\begin{aligned}
f_{C_\Gamma}(C_\Gamma) &= \frac{(1+\Gamma_n)^{-1-\kappa}\ e^{\frac{-1}{\theta(1+\Gamma_n)}}}{\Gamma(\kappa)\theta^\kappa\ \frac{N}{\log(2)\ (1+\Gamma_n)}} \Bigg|_{\Gamma_n = 2^{C_\Gamma/N}-1} \\
&= \frac{e^{-\frac{2^{-C_\Gamma/N}}{\theta}} \left(\frac{2^{-C_\Gamma/N}}{\theta}\right)^k \log(2)}{N\Gamma(k)},
\end{aligned} \tag{45}$$

The outage probability of the system associated with a given transmission rate is defined as the probability that the random variable C_{Γ_n} falls below an arbitrary data rate value, which is named as R_{out}. Accordingly, the outage probability for the GFDM system is therefore given by

$$\begin{aligned}
P_{\text{out}} &= P[C_\Gamma < R_{\text{out}}] \\
&= F_{C_\Gamma}(R_{\text{out}})
\end{aligned} \tag{46}$$

where $F_{C_\Gamma}(C_\Gamma)$ is the cumulative distribution of C_{Γ_n} defined by

$$F_{C_\Gamma}(C_\Gamma) = \int_\infty^{R_{\text{out}}} f_{C_\Gamma(C_\Gamma)}\ \mathrm{d}C_\Gamma \tag{47}$$

In order to solve the (47), we use the following variable substitution: $t = \frac{2^{\frac{-C_\Gamma}{N}}}{\theta}$ in (45). So, $\mathrm{d}t = \frac{-2^{-C_\Gamma/N}}{N\ \theta}\log(2)\ \mathrm{d}C_\Gamma$.

$$F_{C_\Gamma}(C_\Gamma) = \int_{\frac{2^{-C_\Gamma/N}}{\theta}}^{\infty} \left(e^{-t}\ t^{\kappa-1} \right) \mathrm{d}t = \frac{\Gamma\left(\kappa, \frac{2^{\frac{-C_\Gamma}{N}}}{\theta}\right)}{\Gamma(\kappa)}, \tag{48}$$

where the function $\Gamma(a,x) \equiv \int_x^\infty t^{a-1}e^{-t}\mathrm{d}t$ is the upper incomplete Gamma function.

VI. Performance Analysis

To validate the analytical formulations of the achievable sum rate and outage capacity defined in (39) and (46), we employ Monte Carlo simulation to demonstrate the accuracy of the proposed models. The simulation considers different parameters for the GFDM system, namely the prototype filter defined by a root raised cosine (RRC) with a specific roll-off factor, and the number of sub-carriers and symbols. The channel is modeled as a FSFC, for different sizes of the L, power delay profile modeled by $\sigma_m^2 = e^{-0.2m}$, $m = 1,\ldots,L$. The power transmission for data symbols (σ_d^2) is equal to 1. So, the SNR values ($p = \sigma_d^2/\sigma_v^2$) depend only of the noise variance.

A. Achievable sum rate results

Figure 1 presents the achievable sum rate for some number of sub-carriers as $K = 8, 32, 128$, number of sub-symbols as $S = 3, 5$, the roll-off factors $= 0.1, 0.9$, and the number of channels steps is $L = 2$. In all cases, the analytical approximation (represented by lines) matches with high accuracy with the Monte Carlo simulation (represented by markers), indicating the effectiveness of the proposed approach.

As the performance analysis itself, the achievable sum rate is presented as a function of the SNR (p) using a logarithmic scale in the achievable sum rate axis. The greater the $N = S.K$, the higher the achievable sum rate value. For example, when the SNR is 30 dB the achievable sum rate for the case with K=8 and S=3 is less than 100 bps/Hz. For the same SNR value, the achievable sum rate for K=128 and S=5 is approximately 400 bps/Hz. Based on this result, we can conclude that the mathematical model described in (39) is approximating the achievable sum rate with acceptable accuracy in scenarios using a roll-off=0.1 and roll-off=0.9.

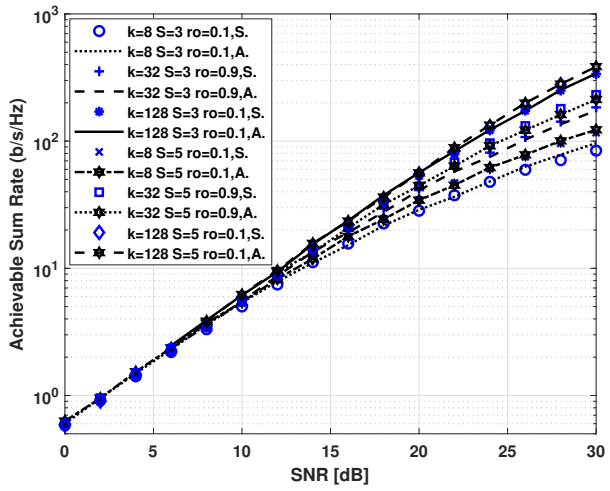

Fig. 1. Simulated and analytic achievable sum rate for GFDM for different values of k,S, roll-off, and L. The abbreviations S. and A. mean simulation and analytical respectively.

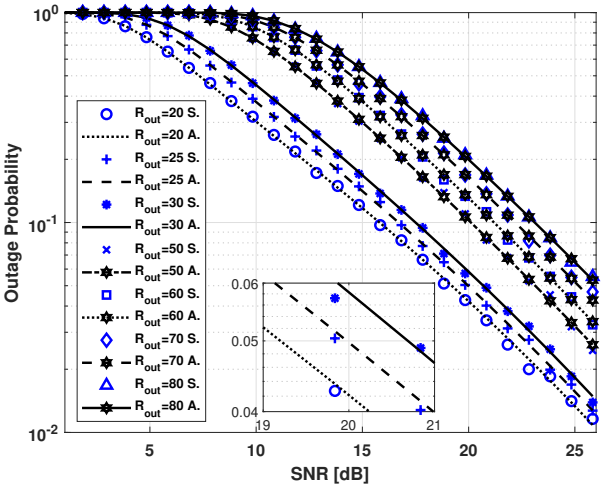

Fig. 2. Probability of outage versus SNR for different values of R_{out} for GFDM ($S = 3$, $K = 32$, $L = 2$) with Roll-off= 0.9. Every R_{out} is in bps/Hz, and the abbreviations S. and A. means simulation and analytical, respectively.

B. Outage results

We considered the following GFDM parameters: $K = 32$, $S = 3$, $L = 2$, and roll-off= 0.1. Many curves were generated based on the assumption that an arbitrary data rate is fixed. These data rates vary from 20 bps/Hz until 80 bps/Hz. As less the value of the data rate, much is the chance of a specific scenario to be in outage. For example, for a $R_{\text{out}} = 20$ bps/Hz and a SNR value of 10 dB the outage probability is equal to 0.3. In the same analyse point, for a $R_{\text{out}} = 80$ bps/Hz the outage probability is increased to 0.95.

VII. Conclusion and Future Works

In this paper, we studied the achievable sum rate and the outage for a GFDM system employing MMSE receivers over FSFC based on a Gamma-distribution approximation for the random variable that define the SINR. This approximation was employed to compute the achievable sum rate and the outage capacity in closed-form. Our numerical results showed the proposed analytical models provide a high accuracy for different GFDM parameters and channel conditions. Our numerical results showed, for instance, that the outage probability when the SNR= 20 for the $R_{\text{out}} = 25$ bps/Hz is less than 5%. As future works, we plan to extend this work to more performance metrics, providing a thorough comparison of the GFDM and other techniques as OFDM.

Acknowledgements

This paper is supported by Academy of Finland via: (a) ee-IoT project n.319009, (b) FIREMAN consortium CHIST-ERA/n.326270, and (c) EnergyNet Research Fellowship n.321265/n.328869.

References

[1] G. Wunder, P. Jung, M. Kasparick, T. Wild, F. Schaich, Y. Chen, S. T. Brink, I. Gaspar, N. Michailow, A. Festag, L. Mendes, N. Cassiau, D. Ktenas, M. Dryjanski, S. Pietrzyk, B. Eged, P. Vago, and F. Wiedmann, "5GNOW: non-orthogonal, asynchronous waveforms for future mobile applications," *IEEE Communications Magazine*, vol. 52, no. 2, pp. 97–105, February 2014.

[2] N. Michailow, M. Matthé, I. S. Gaspar, A. N. Caldevilla, L. L. Mendes, A. Festag, and G. Fettweis, "Generalized frequency division multiplexing for 5th generation cellular networks," *IEEE Transactions on Communications*, vol. 62, no. 9, pp. 3045–3061, 2014.

[3] M. Towliat and S. M. J. A. Tabatabaee, "GFDM Interference Mitigation Without Noise Enhancement," *IEEE Communications Letters*, vol. 22, no. 5, pp. 1042–1045, 2018.

[4] S. Han, Y. Sung, and Y. H. Lee, "Filter Design for Generalized Frequency-Division Multiplexing," *IEEE Transactions on Signal Processing*, vol. 65, no. 7, pp. 1644–1659, April 2017.

[5] D. Carrillo, S. Kumar, G. Fraidenraich, and L. L. Mendes, "Bit Error Probability for MMSE Receiver in GFDM Systems," *IEEE Communications Letters*, vol. 22, no. 5, pp. 942–945, May 2018.

[6] C. Shin, R. W. Heath, and E. J. Powers, "Non-Redundant Precoding-Based Blind and Semi-Blind Channel Estimation for MIMO Block Transmission With a Cyclic Prefix," *IEEE Transactions on Signal Processing*, vol. 56, no. 6, pp. 2509–2523, June 2008.

[7] S. Tiwari, S. S. Das, and K. K. Bandyopadhyay, "Precoded Generalized Frequency Division Multiplexing System to Combat Intercarrier Interference: Performance Analysis," *IET Communications*, vol. 9, no. 15, pp. 1829 – 1841, May 2015.

[8] A. Paulraj, R. Nabar, and D. Gore, *Introduction to space-time wireless communications*. Cambridge university press, 2003.

[9] P. Li, D. Paul, R. Narasimhan, and J. Cioffi, "On the Distribution of SINR for the MMSE MIMO Receiver and Performance Analysis," *IEEE Trans. Inf. Theory*, vol. 52, no. 1, pp. 271 – 286, Jan 2006.

[10] R. M. Gray, "Toeplitz and Circulant Matrices: A Review," *Commun. Inf. Theory*, vol. 2, no. 3, pp. 155–239, Aug. 2005.

[11] I. S. Gradshteyn and I. M. Ryzhik, *Table of Integrals, Series, and Products*, 7th ed., San Diego, CA: Academic, 2007.

[12] C. Zhong, M. Matthaiou, A. Huang, and Z. Zhang, "On the sum rate of MIMO Nakagami-m fading channels with MMSE receivers," in *2012 IEEE 7th Sensor Array and Multichannel Signal Processing Workshop (SAM)*, June 2012, pp. 49–52.

[13] M. Abramowitz and I. Stegun, *Handbook of Mathematical Functions*, New York, NY: Dover, 1972.

[14] A. Maaref and S. Aissa, "Closed-form expressions for the outage and ergodic Shannon capacity of MIMO MRC systems," *IEEE Transactions on Communications*, vol. 53, no. 7, pp. 1092–1095, July 2005.

[15] P. Wijesinghe, U. Gunawardana, and R. Liyanapathirana, "An Efficient Algorithm for Capacity and Outage Probability Estimation in MIMO Channels," *IEEE Communications Letters*, vol. 15, no. 6, pp. 644–646, June 2011.